Research Paper

CCNA2 and KIF23 are molecular targets for the prognosis of adenoid cystic carcinoma

Yongbin Di[1,*], Haolei Zhang[2,*], Bohao Zhang[2], Tianke Li[3,*], Dan Li[2,*]

[1]Department of Stomatology, The First Hospital of Hebei Medical University, Shijiazhuang, Hebei 050030, P.R. China
[2]Department of Otolaryngology, Head and Neck Surgery, The First Hospital of Hebei Medical University, Shijiazhuang, Hebei 050030, P.R. China
[3]Department of Stomatology, The Fourth Hospital of Hebei Medical University, Shijiazhuang, Hebei 050011, P.R. China
[*]Equal contribution

Correspondence to: Tianke Li, Dan Li; **email:** litianb112@163.com, https://orcid.org/0000-0002-8822-4775; li1201192021@163.com, https://orcid.org/0009-0000-3204-4700
Keywords: CCNA2, KIF23, prognosis, adenoid cystic carcinoma, bioinformatics
Received: June 2, 2023 **Accepted:** December 12, 2023 **Published:** April 2, 2024

ABSTRACT

Objective: Adenoid cystic carcinoma (ACC) is a tumor type derived from glands. However, relationship between CCNA2 and KIF23, and adenoid cystic carcinoma remains unclear.
Methods: GSE36820 and GSE88804 profiles for ACC were obtained from the Gene Expression Omnibus (GEO). Differentially expressed genes (DEGs) were identified, and Weighted Gene Co-expression Network Analysis (WGCNA) was conducted. Subsequently, the construction and analysis of protein–protein interaction (PPI) network, functional enrichment analysis, and Gene Set Enrichment Analysis (GSEA) were performed. A gene expression heat map was generated to visually depict the expression difference of core genes between adenoid cystic carcinoma and normal samples. TargetScan was employed to identify miRNAs that regulated central DEGs. Western blotting (WB) was conducted for cell verification.
Results: A total of 885 DEGs were identified. GO and KEGG analyses revealed their main enrichment in responses to chemical stimuli, cell proliferation, tissue development, and regulation of cell proliferation. The GO and KEGG results indicated significant enrichment in aldosterone-regulated sodium reabsorption, the cell cycle, and the PPAR signaling pathway. Notably, core genes (CCNA2 and KIF23) were found to be highly expressed in Adenoid Cystic Carcinoma samples and expressed at low levels in normal samples. WB validated the overexpression of CCNA2 and KIF23 in the Adenoid Cystic Carcinoma group, confirming the protein-level changes associated with cell cycle, metastasis, apoptosis, and inflammatory factors in Adenoid Cystic Carcinoma groups with gene overexpression and knockout.
Conclusions: CCNA2 and KIF23 exhibit high expression levels in ACC, suggesting their potential role as molecular targets for this malignancy.

INTRODUCTION

Adenoid cystic carcinoma (ACC) is a common malignant epithelial tumor of the lacrimal gland, and it is also the most malignant. It is prone to local recurrence and distant metastasis [1]. The tumor consists of basal cells with small, angular, deeply stained nuclei and sparse cytoplasm, arranged into three

prognostic patterns: sieve, tubular and solid [2]. Adenoid cystic carcinoma is also known as a cylindrical tumor or cylindrical adenocarcinoma. The incidence of these tumors is almost the same in any decade of adulthood [3]. Salivary and lacrimal glands are the most common sites for this type of tumor, making it the most common malignancy of minor salivary glands and the parotid gland [4]. ACC can also be found in the glands of the nasal meatus and tracheobronchial trees [5]. Adenoid cystic carcinoma is characterized by late recurrence, so clinical follow-up should be extended for at least 15 years. The best treatment is typically considered to be surgery combined with postoperative radiotherapy to optimize control of local disease. However, the rate of late local recurrence and distant metastasis remains high and may occur decades after the initial diagnosis [6, 7]. Therefore, active exploration of prognostic indicators and key therapeutic targets for ACC is warranted.

As an integral part of the field of life science, bioinformatics has consistently remained at the forefront of life science and technology research. In recent years, China's biotechnology has developed by leaps and bounds, and bioinformation resources have also grown explosively. Bioinformatics reveals the biological significance represented by big data, which is a bridge between data and clinic. Represented by the analysis and reporting of gene detection data, bioinformatics plays a role in the tumor treatment [8, 9].

CCNA2 functions as a pivotal regulatory factor in the cell cycle, encoding a protein essential for orchestrating cell division. High expression of CCNA2 has been implicated in the initiation and progression of various cancers, including breast cancer and lung cancer. Jiang [10] employed bioinformatics methods were employed to analyze the differential expression of CCNA2 across diverse tumor types, utilizing data from multiple databases. The results revealed significant disparities in CCNA2 expression between tumor tissues and corresponding normal tissues. Notably, CCNA2 emerges as a key factor influencing the prognosis of various cancer types, particularly clear cell renal cell carcinoma (ccRCC), and mutations in CCNA2 are prevalent across divers cancer types.

KIF23 is a gene intricately involved in cell mitosis, and its encoded protein plays a crucial role in the final stages of cell division. High levels of KIF23 expression have been correlated with an unfavorable prognosis and tumor invasiveness in various cancers, including breast cancer, lung cancer, and colon cancer. In a study conducted by Gao [11] bioinformatics methods were employed to scrutinize the expression levels of KIF23 mRNA in pancreatic tumor tissues compared to normal pancreatic tissues. The findings revealed a pronounced upregulation of KIF23 mRNA in pancreatic tumor tissues, and a direct association was observed between high KIF23 expression and poor prognosis. Furthermore, the study demonstrated that the inhibition of KIF23 through knockdown approaches could effectively impede the proliferation of pancreatic cells. While some studies have indicated that CCNA2 and KIF23 may play promoting roles in certain cancers, their specific relationship with ACC remains incompletely elucidated. *t* is noteworthy that different genes may exert varying effects in different diseases.

Therefore, the objective of this study was to investigate the core genes distinguishing adenoid cystic carcinoma from normal tissues through the application of bioinformatics techniques. The study validated the significant role of CCNA2 and KIF23 in adenoid cystic carcinoma by analyzing public datasets and further confirmed these findings through basic cell experiments.

METHODS

Adenoid cystic carcinoma dataset

In this study, we downloaded Adenoid Cystic Carcinoma datasets GSE36820 and GSE88804 from the gene expression omnibus (GEO) database (http://www.ncbi.nlm.nih.gov/geo/), which were generated using the GPL570 and GPL6244 platforms. GSE36820 comprises 11 Adenoid Cystic Carcinoma samples and 3 normal samples, while GSE88804 includes 13 Adenoid Cystic Carcinoma samples and 7 normal samples. These datasets were utilized for the identification of differentially expressed genes (DEGs).

DEG selection

The R package "limma" was utilized for probe summarization and background correction in GSE36820 and GSE88804. The Benjamini-Hochberg method was applied to adjust the original *p*-values, and the fold change (FC) was calculated using the false discovery rate (FDR). The DEG cutoff criteria were set as $p < 0.05$ and FC >2. Subsequently, a volcano plot was generated to visualize the results.

Weighted gene co-expression network analysis (WGCNA)

First, using the gene expression profiles from GSE88804, we calculated the Median Absolute Deviation (MAD) for each gene, and subsequently excluded the lower 50% of genes with the smallest MAD. The "goodSamplesGenes" function of the R

package WGCNA was used to eliminate outlier genes and samples. Subsequently, a scale-free co-expression network was constructed using WGCNA. In the initial step, a Pearson correlation matrix and average linkage method were applied to all pairwise genes. This was followed by the creation of a weighted adjacency matrix using a power function A_mn = |C_mn|^β, where C_mn represents the Pearson correlation between Gene_m and Gene_n, and A_mn denotes the adjacency relationship between Gene_m and Gene_n. The parameter β serves as a soft-thresholding parameter that accentuates strong correlations and while attenuating weak ones. A power of 14 was chosen. The adjacency relationships were transformed into the Topological Overlap Matrix (TOM), quantifying the connectivity of a gene in the network as the sum of adjacency relationships with all other genes. Subsequently, dissimilarity (1-TOM) was calculated. Hierarchical clustering was performed based on TOM-based dissimilarity to categorize genes into modules of co-expressed genes. The minimum module size for the gene dendrogram was set at 30, and a sensitivity of 3 was applied to cut the dendrogram. The modules were further merged if their distance was less than 0.25. Importantly, the grey module was designated to include genes that could not be assigned to any other module.

Protein-protein interaction (PPI) network construction and analysis

The STRING database compiles, scores, integrates, and supplements protein-protein interaction information from various diverse sources. In this study, the list of differentially expressed genes was input into the STRING database to construct a PPI network for predicting core genes with a confidence score >0.4. The Cytoscape software was utilized for the visualization and prediction of core genes within the PPI network. Initially, the PPI network was imported into Cytoscape, and modules with the highest connectivity were identified using the MCODE algorithm. The ten genes with the most connections were determined using Maximum Clique Centrality (MCC) and Maximum Network Connectivity (MNC), and the intersection of these genes was visualized and exported as the list of core genes.

Functional enrichment analysis

Gene Ontology (GO) and Kyoto Encyclopedia of Genes and Genomes (KEGG) analyses are computational methods for evaluating gene functions and biological pathways. In this study, the list of differentially expressed genes obtained from the Venn diagram was input into KEGG database via the KEGG REST API (https://www.kegg.jp/kegg/rest/keggapi.html) to retrieve the latest KEGG Pathway gene annotations. These annotations served as the background, and the genes were mapped to the background set. Enrichment analysis was conducted using the R package clusterProfiler (version 3.14.3) to obtain results for gene set enrichment. Additionally, GO annotations of genes were obtained from the R package org.Hs.eg.db (version 3.1.0). The analysis settings included a minimum gene set of 5 and a maximum gene set of 5000, with a *P*-value threshold of <0.05 and a false discovery rate (FDR) of <0.25, indicating statistical significance. Moreover, the Metascape database was employed for comprehensive gene list annotation and analysis resources, and the results were visualized and exported.

Gene set enrichment analysis (GSEA)

For Gene Set Enrichment Analysis (GSEA), the samples were categorized into two groups (Adenoid Cystic Carcinoma and normal samples), and the gene expression profiles were aligned with the Molecular Signatures Database (MSigDB) subset c2.cp.kegg.v7.4.symbols.gmt to assess relevant pathways and molecular mechanisms. GSEA software (version 3.0) was acquired from the GSEA website (http://software.broadinstitute.org/gsea/index.jsp), and the analysis was executed based on gene expression profiles and phenotype grouping, with a minimum gene set size of 5, maximum gene set size of 5000, 1000 permutations, and significance criteria set at a *P*-value < 0.05 and an FDR <0.25. Additionally, GO and KEGG analyses were performed for the entire genome, separately for GSE36820 and GSE88804.

Gene expression heatmap

We used the R package heatmap to generate heatmaps representing the expression levels of core genes identified by the two algorithms within the PPI network in GSE36820 and GSE88804. These heatmaps visually portray the expression differences of core genes between Adenoid Cystic Carcinoma and normal samples.

miRNA

TargetScan (http://www.targetscan.org/) is an online database utilized for predicting and analyzing miRNAs and their target genes. In our study, TargetScan was employed to screen for miRNAs that regulate the central DEGs.

Western blotting (WB)

We conducted WB verification and divided samples into the Normal group, Adenoid Cystic Carcinoma

group (ACC), Adenoid Cystic Carcinoma oncogene overexpression group (ACC_OE) and Adenoid Cystic oncogene knockout group (ACC_KO).

Total tissue protein was extracted. Tissue blocks were washed 2–3 times with pre-cooled PBS to remove blood stain, cut into small pieces, and placed in a homogenizing tube. Lysate, 10 times the volume of tissue, was added. The homogenized tube was taken out and centrifuged at 12000 rpm for 30 minutes at 4°C. The supernatant was collected after centrifugation. Protein quantification was performed with BCA protein quantification kit, and standard curves were generated with (Thermo, MK3, America). The quantified proteins were separated by SDS-Polyacrylamide gel electrophoresis (SDS-PAGE). The proteins are then transferred to a polyvinylidene fluoride (PVDF) membrane. Then, the film was closed with 5% BSA at room temperature for 1 hour.

After adding CCNA2 antibody (dilution ratio 1:5000, Proteintech, 18202-1-AP, Wuhan, China), KIF23 antibody (dilution ratio 1:1000, Proteintech, 28587-1-AP, Wuhan, China), the corresponding proteins were detected by GAPDH (dilution ratio 1:5000, Proteintech, 10494-1-AP, Wuhan, China). Using GAPDH as the internal reference, CCNA2 antibody was used to detect CCNA2, KIF23 antibody was used to detect KIF23, and other corresponding antibodies were used to detect corresponding proteins. The primary antibody was recovered and washed with TBST three times for 5–10 min each time. The corresponding enzyme labeled second antibody (dilution ratio 1:5000) was added and incubated at room temperature for 60 min. Remove the eluted PVDF film and put it on absorbent paper, slightly blot the liquid above the film, put the film on the Chemiluminescence shelf, add the mixed (Enhanced Chemiluminescence) ECL luminescent liquid, let the liquid completely immersed in the film, after 1 min reaction, put it into the chemiluminescence instrument. Start chemiluminescence according to the preset procedure, save the original image, and then analyze the data with AIWBwell™ analysis software.

Data availability

The datasets generated during and/or analyzed during the current study are available from the corresponding author on reasonable request.

RESULTS

Screening of DEGS

In this study, we identified DEGs in GSE36820 (Figure 1A) and GSE88804 (Figure 1B) datasets. The intersection of these datasets was determined through a Venn diagram, revealing a total of 885 DEGs (Figure 1C).

Functional enrichment analysis

DEGs

We conducted GO and KEGG analysis on the differentially expressed genes. In terms of the Gene Ontology Biological Process (BP) analysis, these genes were predominantly enriched in responses to chemical stimuli, cell proliferation, tissue development, and cell proliferation regulation (Figure 2A). Gene Ontology Cellular Component (CC) analysis indicated, their main enrichment in extracellular region, membrane system, vesicles, and extracellular region part (Figure 2B). Additionally, Gene Ontology Molecular Function (MF) analysis revealed enrichment in anion binding, small molecule binding, drug binding, and molecular function modulator (Figure 2C).

The KEGG analysis results indicated that the target genes were predominantly enriched in the Wnt signaling pathway, PPAR signaling pathway, and salivary secretion (Figure 2D).

GSEA

Furthermore, we performed GSEA enrichment analysis on the entire genome to identify potential enrichments within non-differentially expressed genes and validate the findings from differentially expressed genes. The intersection of enrichment items with the GO and KEGG enrichment items of differentially expressed genes was visualized, primarily showing enrichment in aldosterone-regulated sodium reabsorption, cell cycle, and PPAR signaling pathway. These observations were consistent in GSE36820 (Figure 3A–3D) and GSE88804 (Figure 3E–3H).

Metascape enrichment analysis

In the Metascape enrichment analysis, significant enrichments were observed in GO terms such as mitotic cell cycle, multicellular organismal homeostasis, and positive regulation of the cell cycle (Figure 4A). Furthermore, we constructed enrichment networks with items colored by enrichment and *p*-values (Figure 4B–4D), visually illustrating the associations and confidence levels of various enrichment items.

WGCNA

The selection of the soft-thresholding power is a crucial step in WGCNA analysis. We conducted network topology analysis to determine the optimal soft-thresholding power. In our WGCNA analysis, the

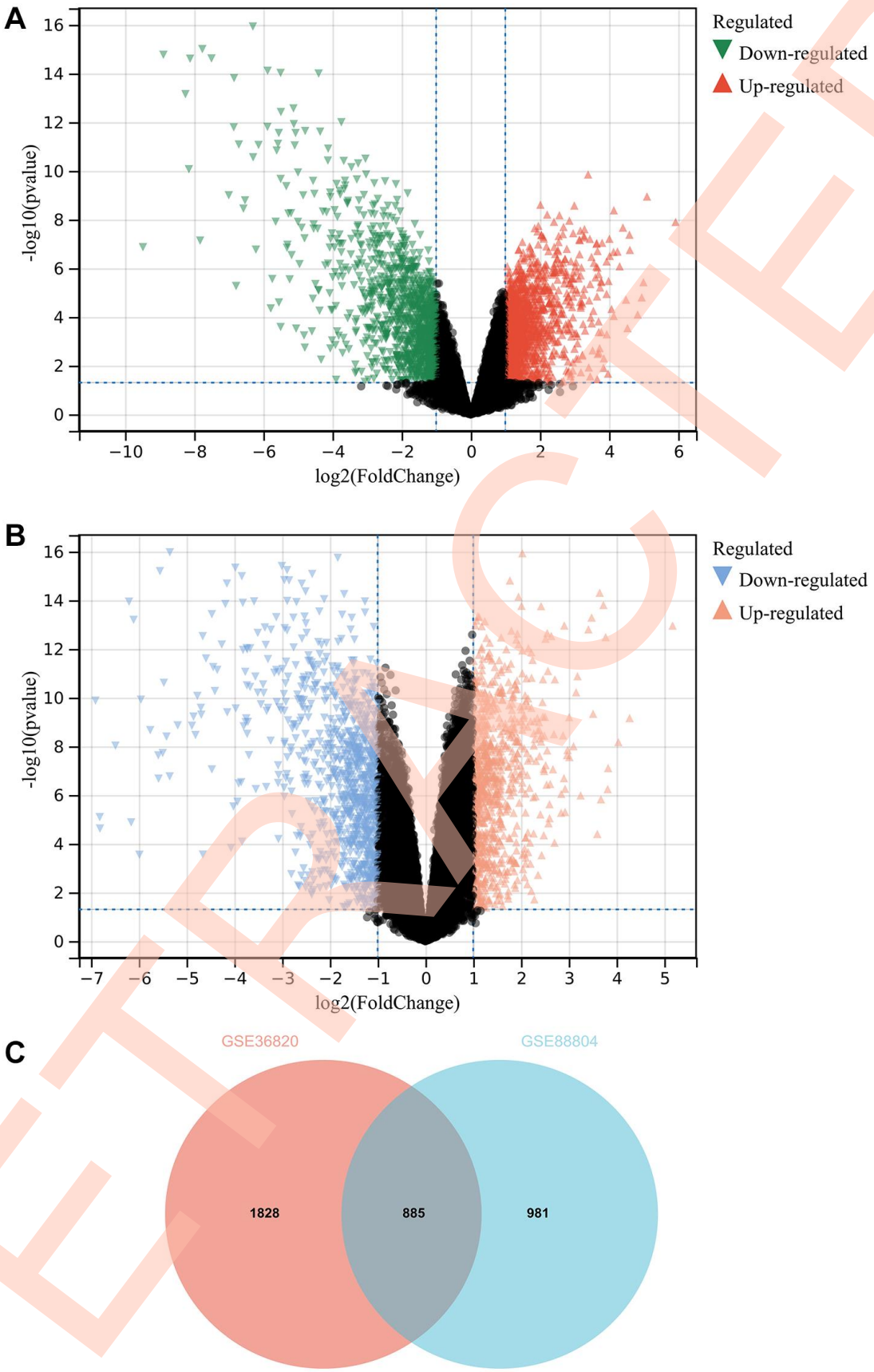

Figure 1. Screening of DEGS. (**A**) Identification of DEGs by GSE36820. (**B**) Identification of DEGs by GSE88804. (**C**) Screening of DEGS. The intersection of Venn diagram, a total of 885 DEGs were identified.

soft-thresholding power was set at 14 (Figure 5A, 5B). Subsequently, we constructed a hierarchical clustering tree encompassing all genes and identified significant modules. Interactions between these modules were then analyzed (Figure 5C, 5D). A heatmap illustrating the module-trait relationships was generated (Figure 6A), along with a scatter plot depicting the relationship between gene significance (GS) and module membership (MM) for hub genes (Figure 6B–6E and Figure 7A–7G).

Moreover, we merged modules with a distance less than 0.25 and calculated the module eigengene (ME) correlation with gene expression to obtain MM. Using the cutoff criterion (|MM| >0.8), we identified 4591 genes with high connectivity as hub genes in clinically significant modules.

We further employed a Venn diagram to integrate WGCNA with DEGs, utilizing it for the construction and analysis of the protein-protein interaction network (Figure 7H).

Protein-protein interaction (PPI) network construction and analysis

The PPI network of DEGs was constructed using the STRING online database and analyzed through Cytoscape software (Figure 8A). Core gene clusters were identified (Figure 8B). Two distinct algorithms were applied to determine hub genes (Figure 9A, 9B). The results were intersected using a Venn diagram (Figure 9C), revealing 10 core genes (TPX2, TTK, NUSAP1, CCNA2, DLGAP5, MELK, NCAPG, PBK, KIF23, KIF11).

Gene expression heatmap

We generated a heatmap to visually represent the expression differences of core genes between Adenoid Cystic Carcinoma and normal samples. Our analysis revealed that core genes (CCNA2, KIF23) exhibited higher expression levels in Adenoid Cystic Carcinoma samples and lower expression levels in normal samples,

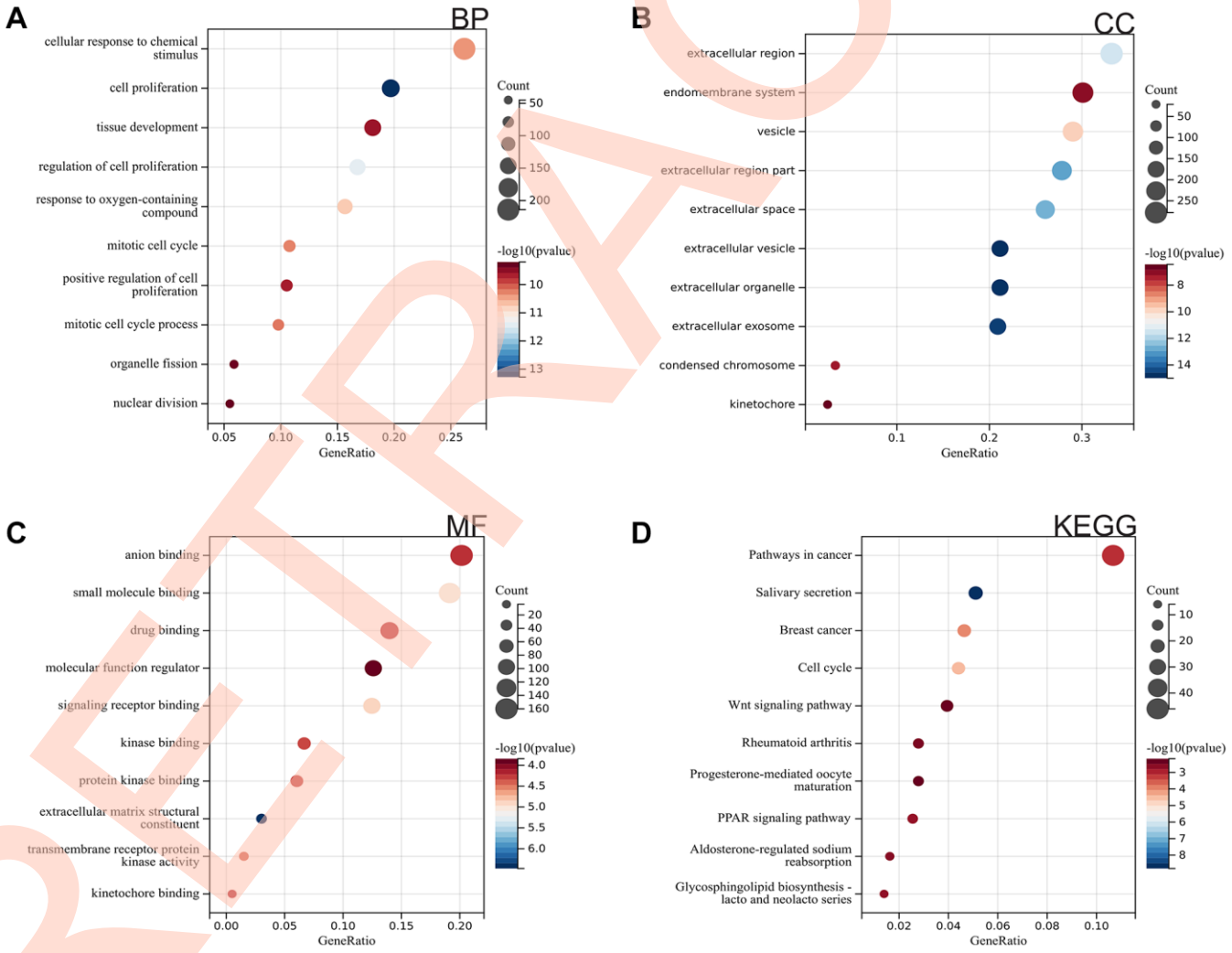

Figure 2. Functional enrichment analysis of DEGs. (**A**) GObp analysis. (**B**) GOcc analysis. (**C**) GOmf analysis. (**D**) KEGG analysis.

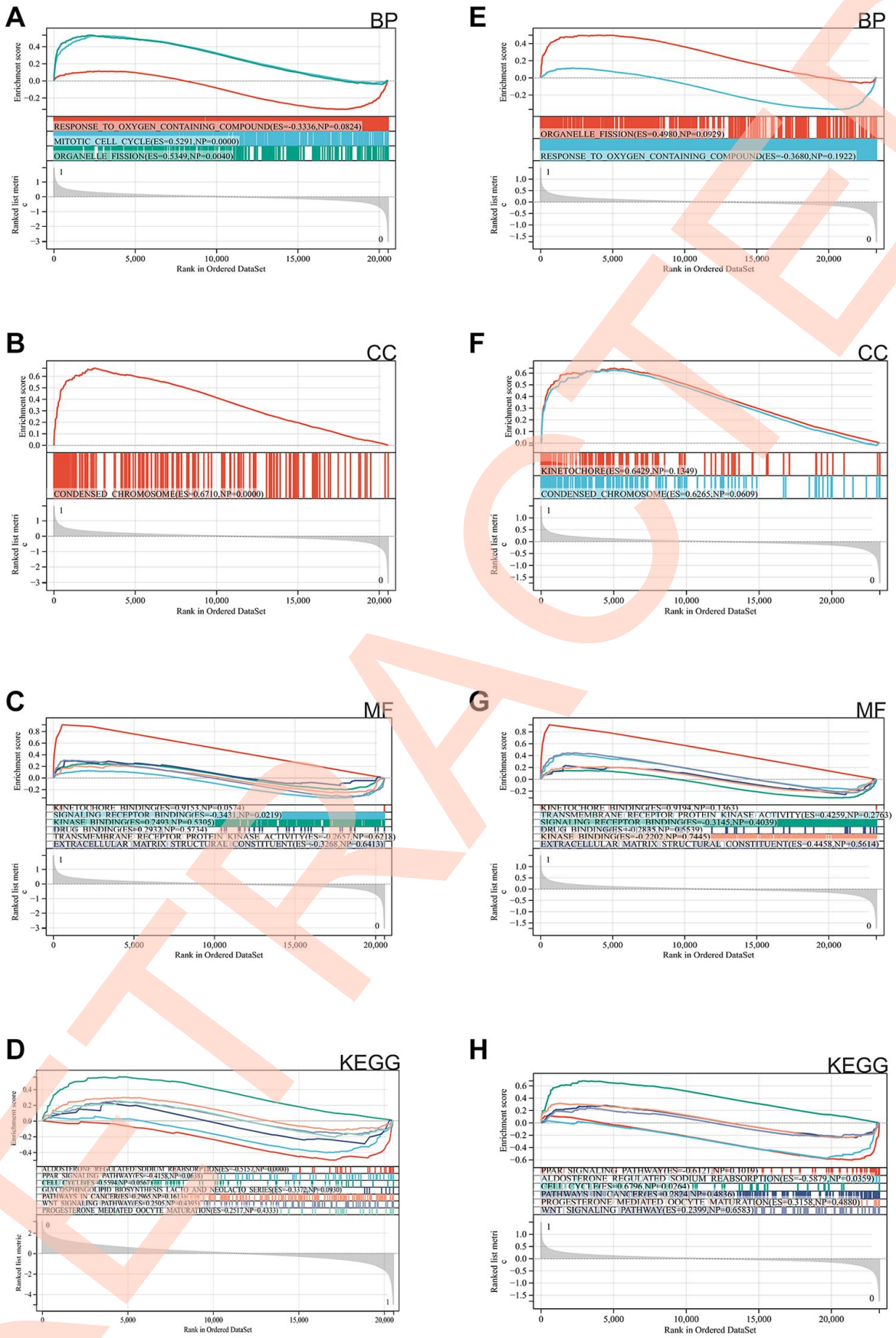

Figure 3. GSEA. (**A**–**D**) GSE36820. (**E**–**H**) GSE88804.

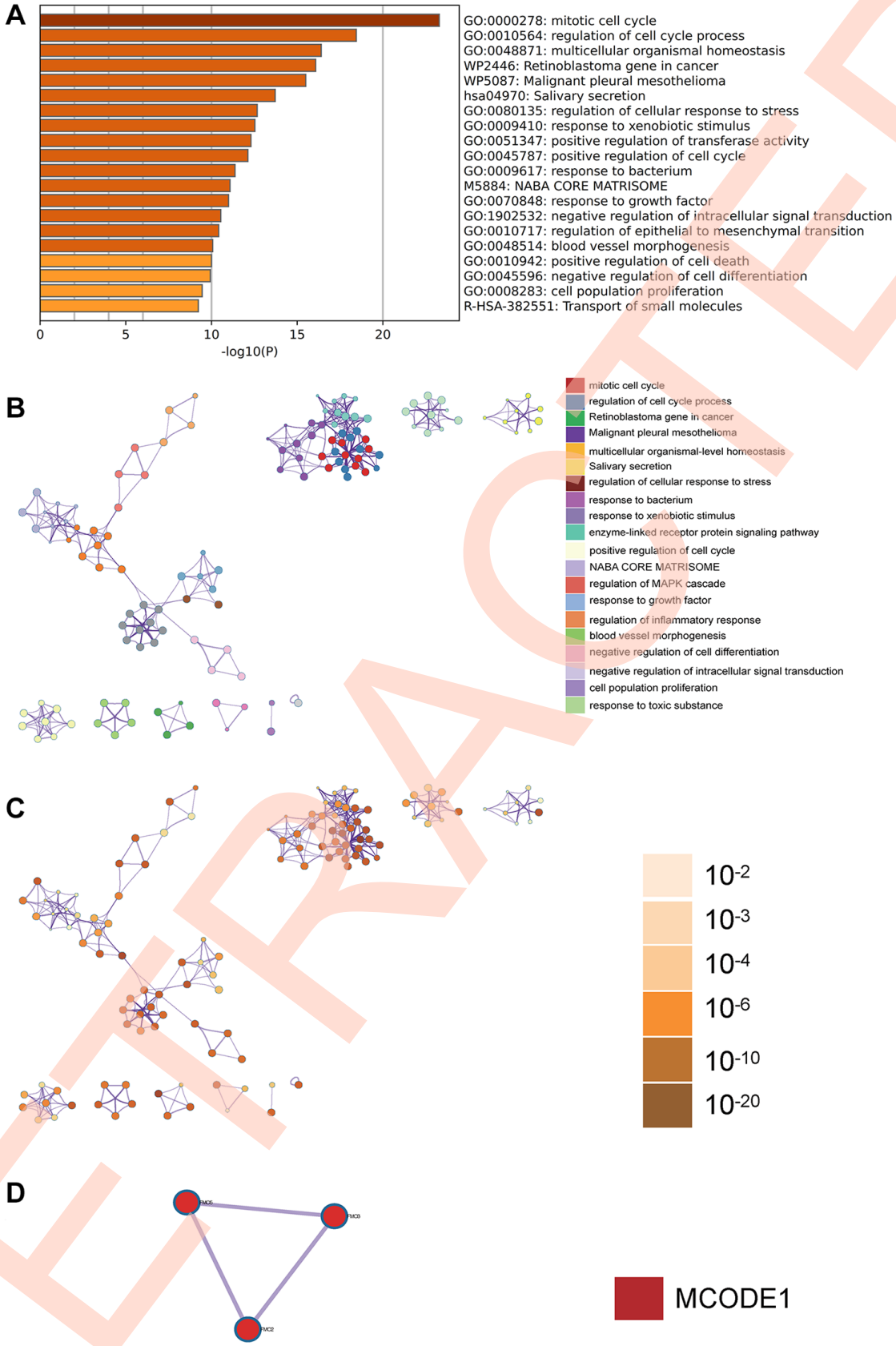

Figure 4. Metascape enrichment analysis. (**A**) GO has positive regulation of mitotic cell cycle, homeostasis in multicellular organisms and cell cycle. (**B**–**D**) Enrichment networks colored by enrichment terms; enrichment networks colored by *p*-values; Metascape enrichment analysis. Visually represent the correlation and confidence of each enrichment project.

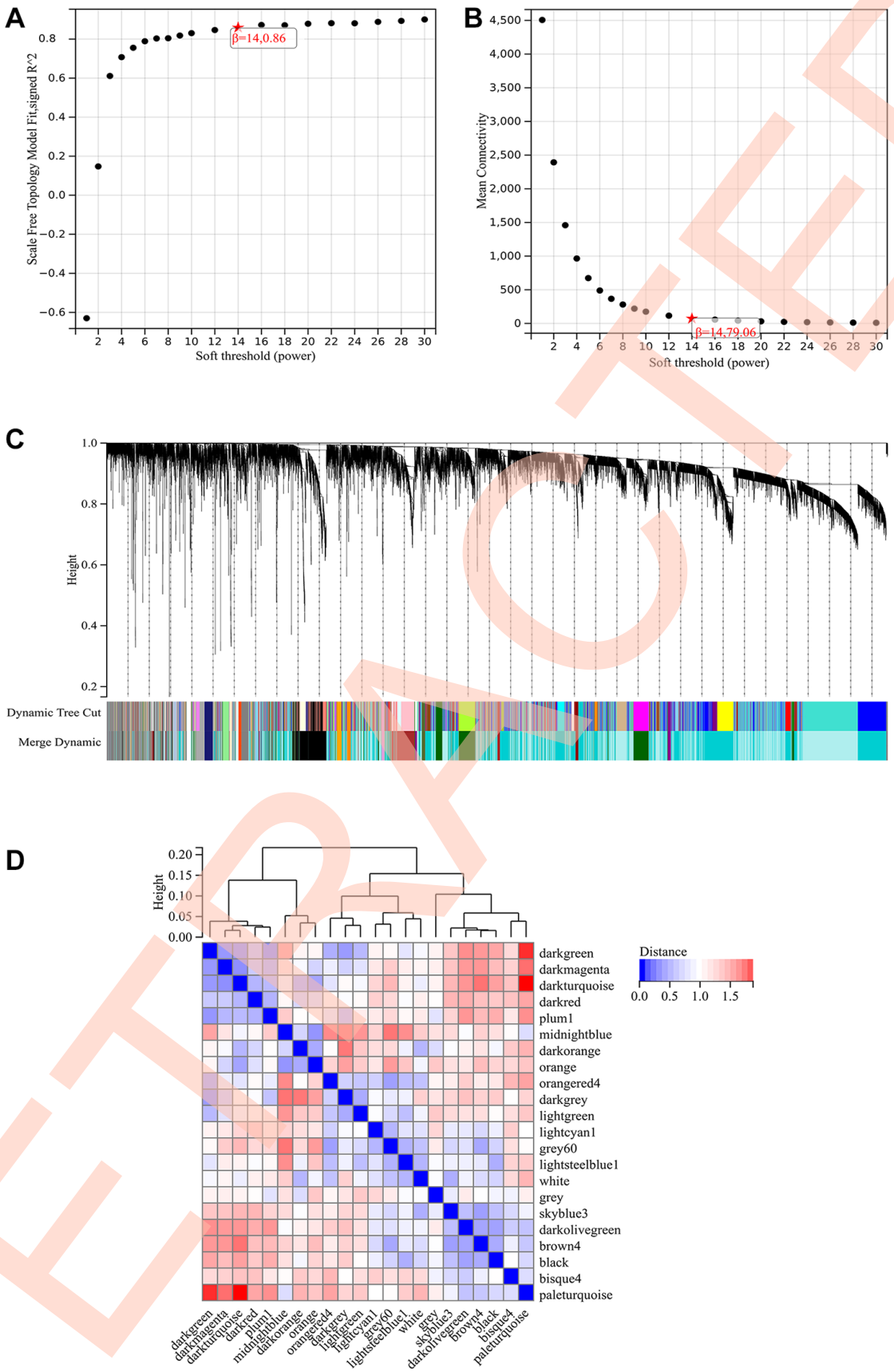

Figure 5. WGCNA. (**A**) β = 14, 0.86. (**B**) β = 14, 79.06. (**C**) A hierarchical clustering tree of all genes is constructed and important modules. (**D**) The interaction between these modules.

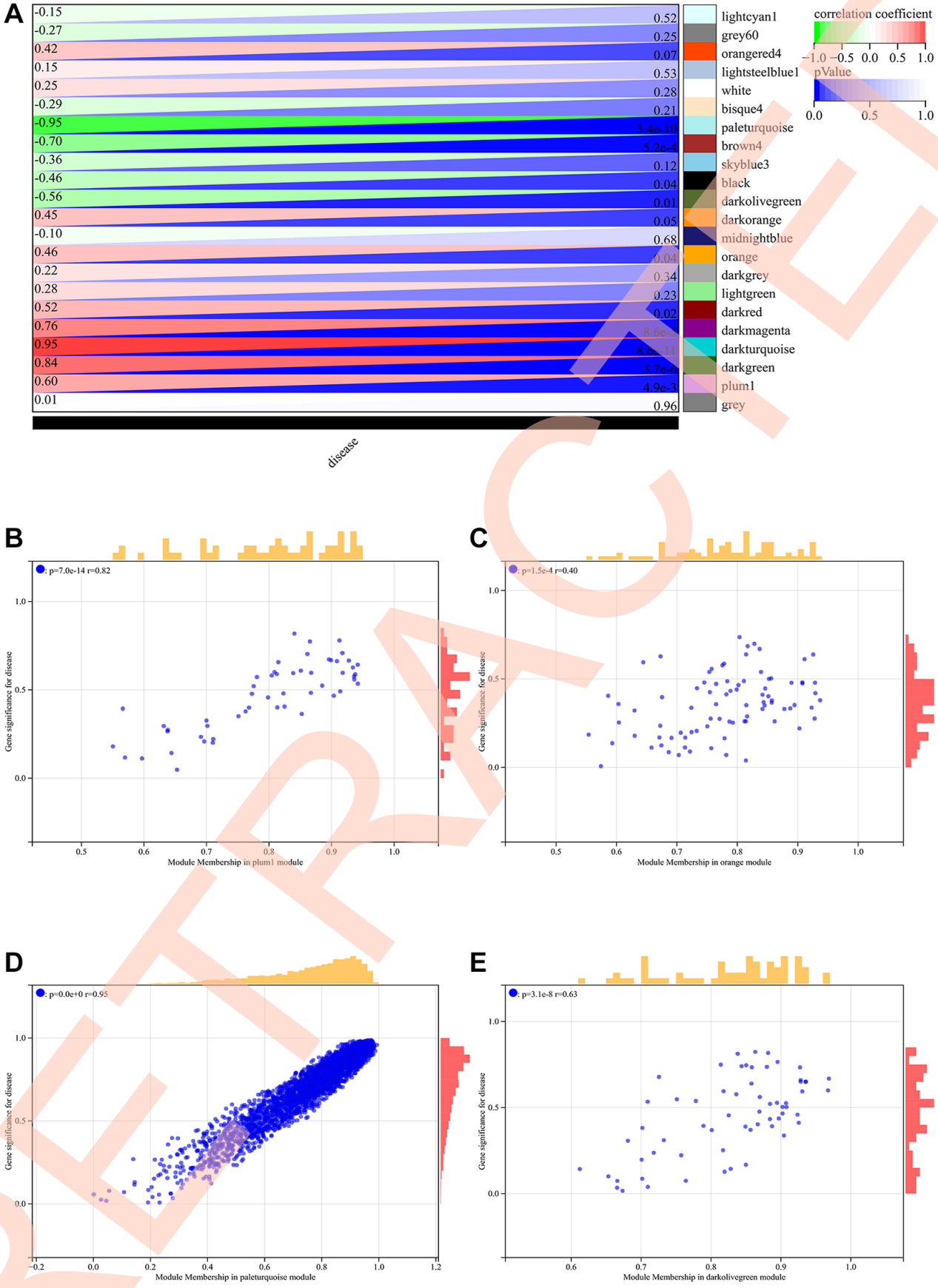

Figure 6. WGCNA. (**A**) The module-phenotypic correlation heat map. (**B–E**) GS-MM correlation scatter map of related hub genes.

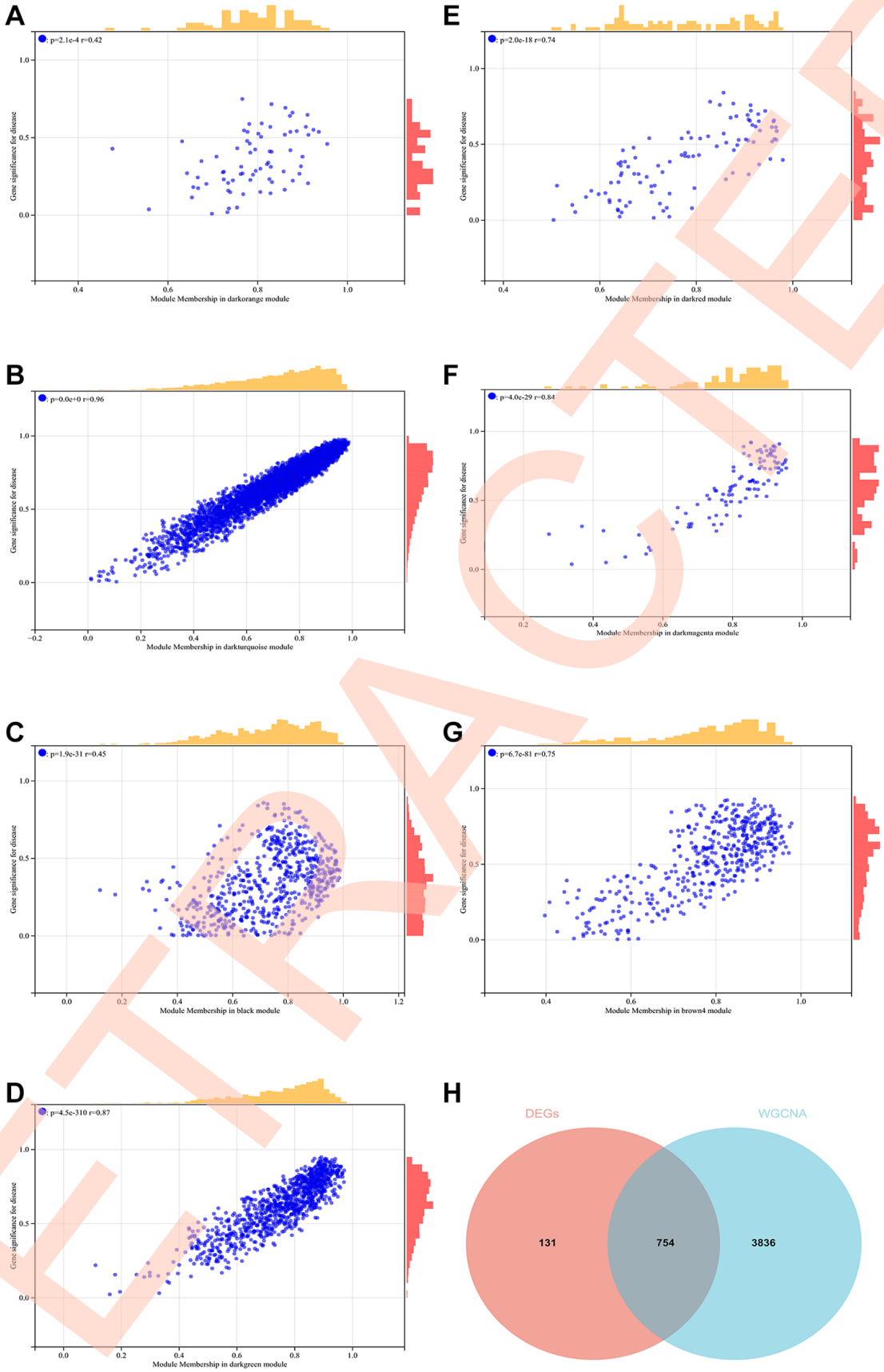

Figure 7. WGCNA. (**A**–**G**) GS-MM correlation scatter map of related hub genes. (**H**) The Venn diagram of the differential genes screened by WGCNA and DEGs and take the intersection to create and analyze the protein-protein interaction network.

indicating their potential regulatory roles (GSE36820 - Figure 10A; GSE88804 - Figure 10B).

Prediction and functional annotation of miRNAs associated with hub genes

In this study, we inputted the list of hub genes into TargetScan to identify relevant miRNAs, thereby enhancing our understanding of gene expression regulation (see Table 1). Our analysis revealed that the miRNAs associated with the CCNA2 gene included hsa-miR-6766-3p, hsa-miR-219a-5p, and hsa-miR-4782-3p, while those associated with the KIF23 gene were hsa-miR-103a-3p and hsa-miR-107.

The protein expression of CCNA2 and KIF23

The Western blot (WB) results demonstrated that the expression levels of CCNA2, KIF23, PML, RARA, CEBPE, BCL2A1, MYC, and DUSP6 were

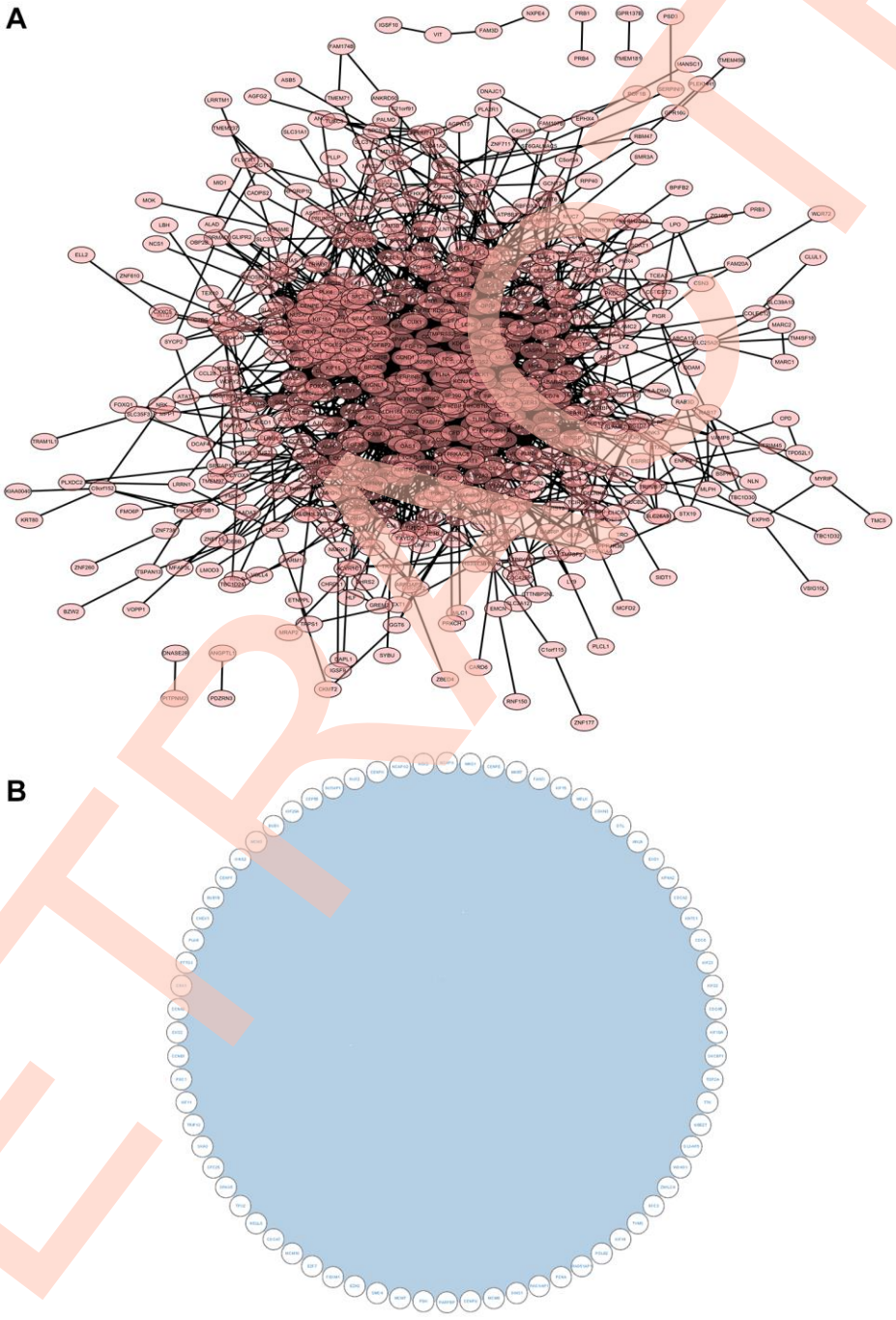

Figure 8. Construction and analysis of protein-protein interaction (PPI) network. (**A**) The PPI network of DEGs. (**B**) Core gene clusters were obtained.

significantly higher in the Adenoid Cystic Carcinoma (ACC) group compared to normal samples ($P < 0.01$). In the ACC_Overexpression (ACC_OE) group, the expression levels were significantly higher than in the ACC group ($P < 0.01$). Conversely, in the ACC_Gene Knockout (ACC_KO) group, the expression levels were significantly lower than in the ACC group ($P < 0.01$) (Figure 11). Regarding cell cycle, metastasis, and apoptosis, the expression of C-Myc, MMP-2, and BCL2 exhibited a consistent pattern across the different groups (Figures 12 and 13).

The inflammatory factor IL-10 exhibited significantly lower expression levels in the ACC group compared to normal samples ($P < 0.01$). In the ACC_OE group, IL-10 expression was markedly higher than in the ACC

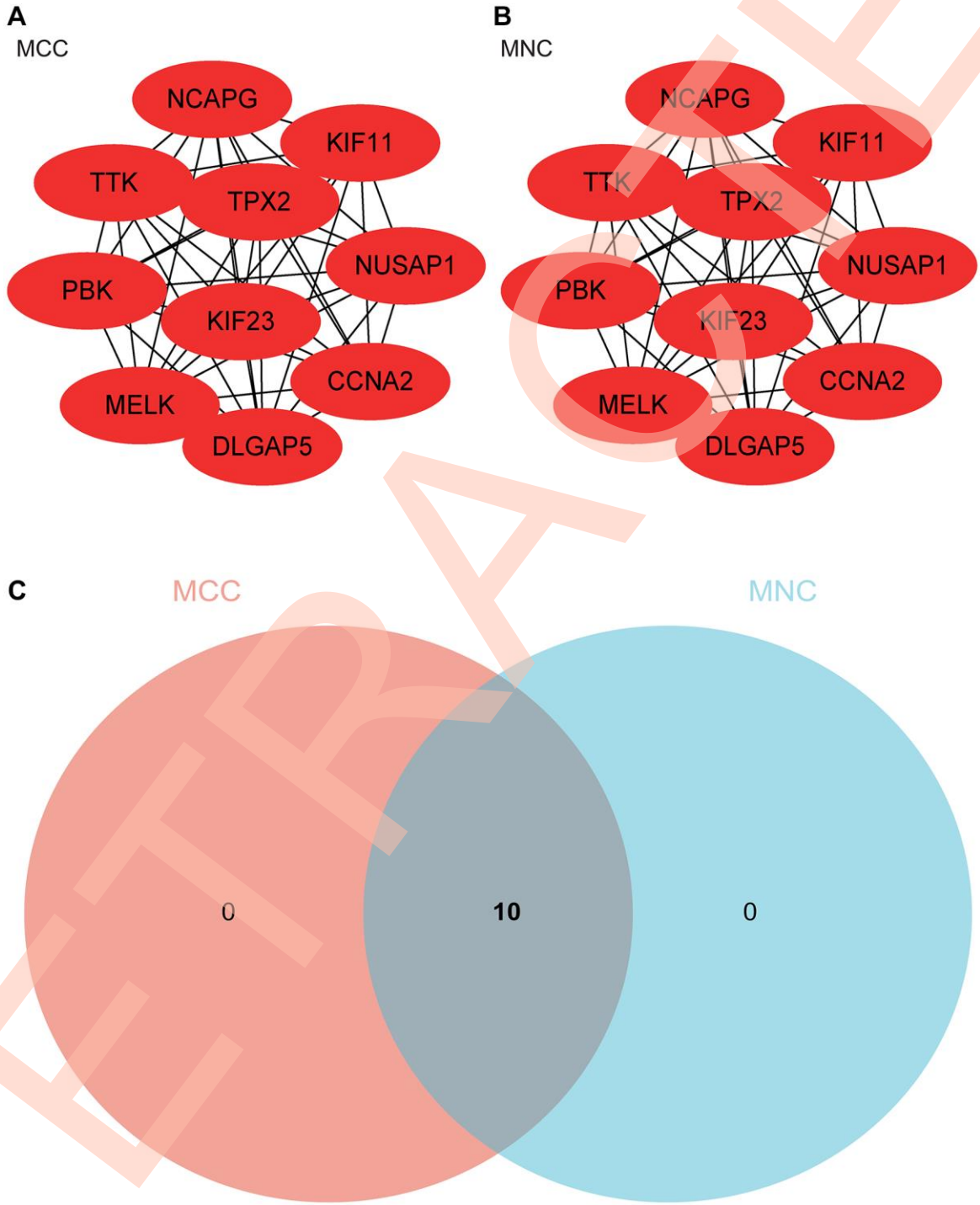

Figure 9. Construction and analysis of protein-protein interaction (PPI) network. (**A**) MCC was used to identify central genes (**B**) MNC was used to identify central genes. (**C**) Venn diagram is drawn and intersected.

group ($P < 0.01$). Conversely, in the ACC_KO group, IL-10 expression was significantly lower than in the ACC group ($P < 0.01$) (Figure 12).

DISCUSSION

ACC is a rare malignant tumor [12–14]. Patients can survive with tumor for a long time. High recurrence rate and distant metastasis are the primary challenges of ACC [15]. ACC exhibits demonstrates to immune checkpoint inhibition owing to its low tumor immunogenicity and the absence ofPD-L1 expression. The key findings of this study uncover high expression levels ofCCNA2 and KIF23 genes in adenoid cystic carcinoma. Elevated expression of CCNA2 and KIF23 genes correlates with a worse prognosis, potentially tied

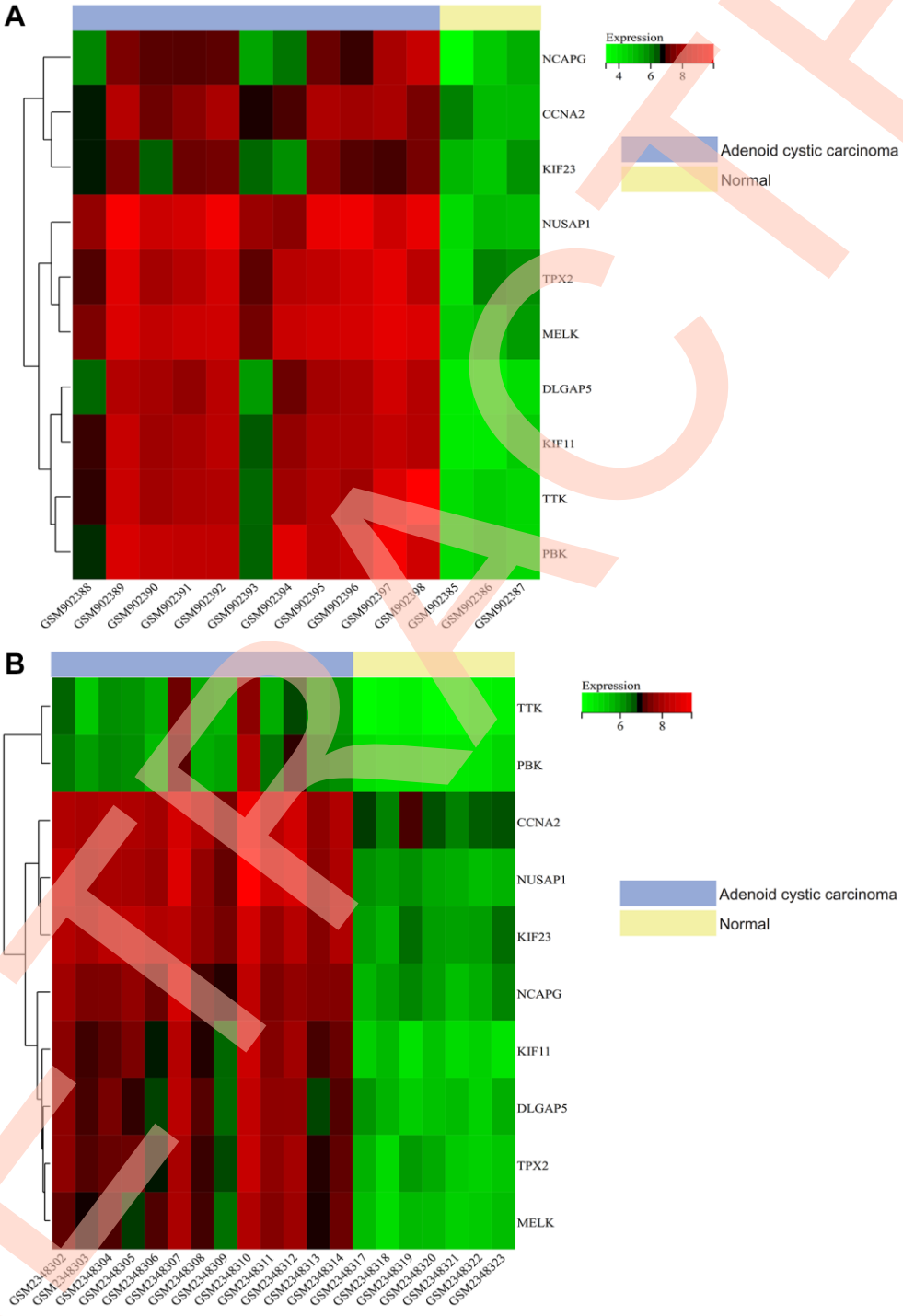

Figure 10. Gene expression heat map. The heat map of the expression of core genes in the samples. (**A**) The result of GSE36820. (**B**) The result of GSE88804.

Table 1. A summary of miRNAs that regulate hub genes.

	Gene	MIRNA		
1	CCNA2	hsa-miR-6766-3p	hsa-miR-219a-5p	hsa-miR-4782-3p
2	KIF23	hsa-miR-103a-3p	hsa-miR-107	

to specific receptors, such as prostate-specific membrane antigen (PSMA), and certain signaling pathways in adenoid cystic carcinoma.

CCNA2, situated in the Q27 region of human chromosome 4, is a member of the highly conserved cyclin family of cell cycle proteins. This protein has been implicated in d the regulation of cell cytoskeleton dynamics and cell movement [16]. Recent studies propose a potential role of CCNA2 in augmenting cancer recurrence and promoting resistance to chemotherapy [17]. Ruan et al. found that CCNA2 can promote epithelial-mesenchymal transition (EMT) in non-small cell lung cancer through integrin αvβ3 signaling [18]. Increased CCNA2 expression is frequently associated with adverse clinical and pathological features across various cancer types [19], leading to a less favorable prognosis. CCNA2 has emerged as a prognostic biomarker, particularly in monitoring tamoxifen efficacy in ER+ breast cancer. Its expression levels may help monitor tamoxifen efficacy and guide personalized treatment [20]. Additionally, CCNA2 expression has been correlated with immune cell levels, including memory CD4+ cells and infiltration of M0 and M1 macrophages, in diverse cancer types. Changes in the immune associated with CCNA2 may favor tumor cell proliferation [21]. Given its role as a cell cycle protein, CCNA2 overexpression

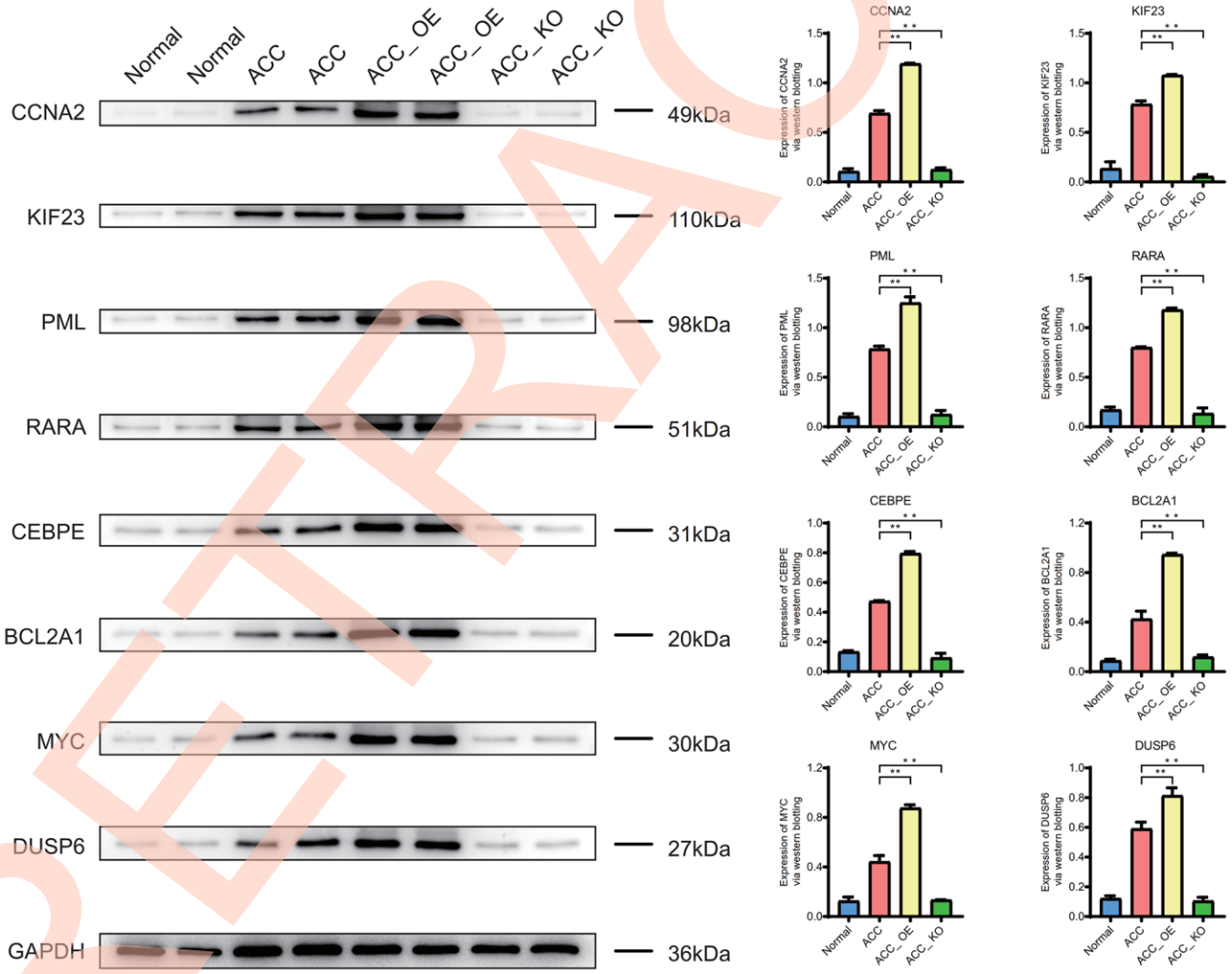

Figure 11. Western blotting. Expression of CCNA2, KIF23, PML, RARA, CEBPE, BCL2A1, MYC, and DUSP6 proteins in ACC group.

may drive tumor cells into cell division phases, contributing to tumor growth and dissemination. Gan et al. have identified CCNA2 as a novel oncogene involved in regulating cancer cell growth and apoptosis [22]. CCNA2 regulates the cell cycle by promoting transitions from G1/S to G2/M phases, thus influencing tumor cell behavior. Furthermore, CCNA2 may act through various signaling pathways, such as promoting migration and inhibit apoptosis in HTR8 cells via the RhoA-ROCK signaling pathway, and enhancing proliferation through the p53 pathway [23].

Cyclin-dependent kinase 2 (CDK2) is a pivotal protein kinase intricately involved in the intricate regulation of

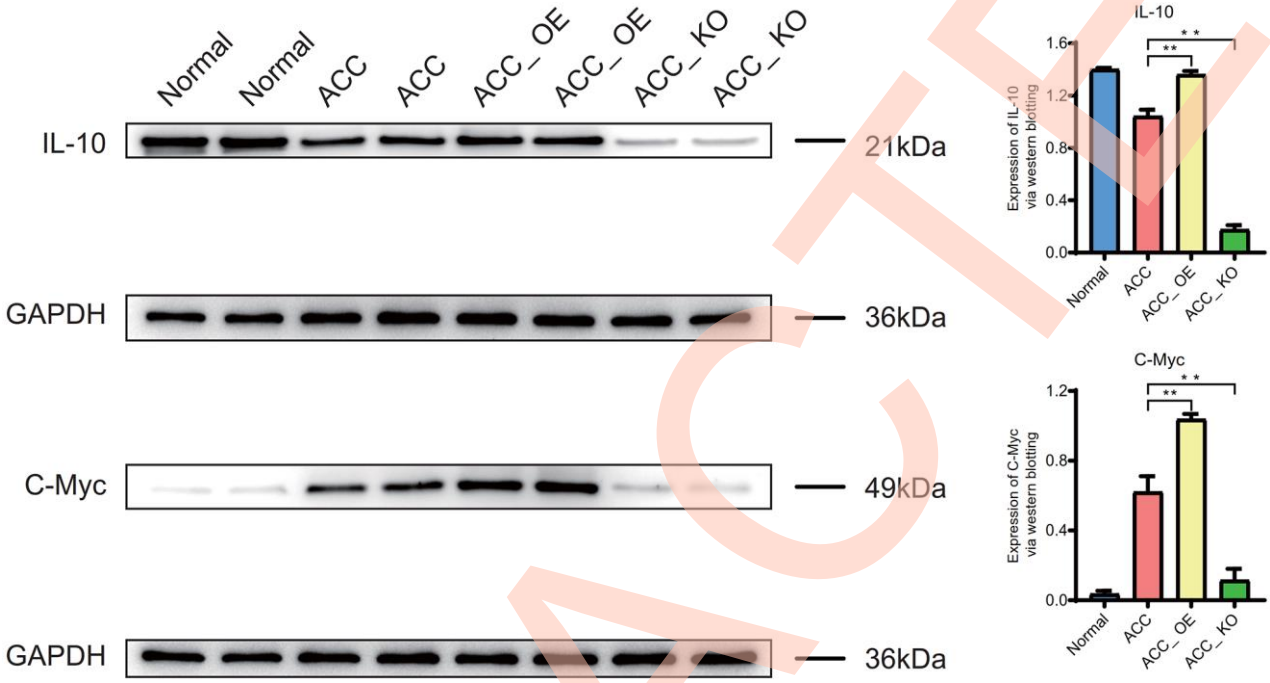

Figure 12. Western blotting. Expression of IL-10 and C-Myc proteins in ACC group.

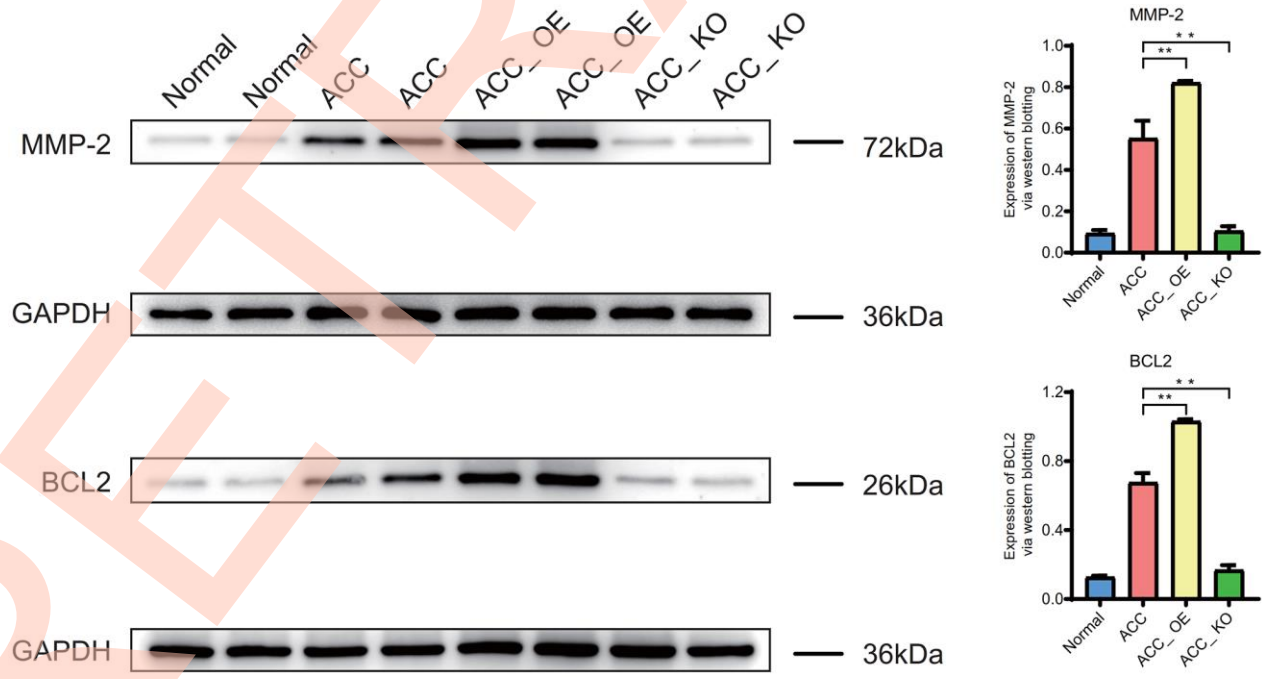

Figure 13. Western blotting. Expression of MMP-2, BCL2 proteins in ACC group.

the cell cycles. It assumes a central role in diverse cellular processes, encompassing DNA damage response, intracellular transport, protein degradation, signal transduction, DNA and RNA metabolism, as well as translation pathways. CDK2 interacts with proteins in these pathways, leading to their phosphorylation [24]. When CDK2 forms an active complex with its regulatory proteins, cyclin E or cyclin A, it becomes a key player in orchestrating cellular processes. Aberrant CDK2 activity can lead to unchecked cell proliferation, emerging as a crucial factor in the growth of cancer cells. The interplay between CDK2 and tumor suppressor genes may compromise the cell's ability to monitor and repair abnormalities, thereby fostering cancer development. Inhibiting CDK2 can induce anti-tumor activity, preventing the division and proliferation of cancer cells [25, 26]. The KEGG analysis conducted in this study reveals that the target genes are predominantly enriched in the Wnt signaling pathway, PPAR signaling pathway, and salivary secretion. These pathways collectively impact the proliferation of adenoid cystic carcinoma cells. Consequently, it is plausible to posit that CCNA2 may play a substantive role in the development of adenoid cystic carcinoma, potentially serving as an oncogene and a promising therapeutic target.

KIF23 is a protein encoded by a human gene and serves as a key regulatory factor in mitosis [27]. This member of the kinesin family, Kinesins family member 23 (KIF23), predominantly localized in cytoplasm and nucleus, playing a significant role in cell mitosis and microtubule-based motility through spindle formation [28]. The protein encoded by the KIF23 gene belongs to motor protein-like protein family, which consists of microtubule-dependent molecular motors responsible for transporting organelles and facilitating chromosomes movement during cell division. KIF23 inhibits the formation of the midbody and cytokinesis, leading to defects in cell division and the formation of multinucleated cells. It actively participates in the development of the cell membrane during the cell division process. Aberrant expression or activity may result in excessive cell proliferation and is associated with the invasion and migration of tumor cells [29]. KIF23 dysfunction leads to mitotic arrest and the appearance of binucleated or multinucleated cells, which in turn leads to tumorigenesis [30].

The study has shown that KIF23 expression is up-regulated in a variety of tumors [31]. Zou confirmed that KIF23 overexpression is associated with the prognosis of breast cancer patients. KIF23 knockout inhibits proliferation and induces apoptosis in drug-resistant breast cancer cells [32]. Colorectal cancer patients exhibiting high KIF23 are associated with a poorer poor prognosis. Yao et al. observed an up-regulation of KIF23 expression in human bladder cancer. The expression levels of KIF23 were found to be correlated with the prognosis and clinicopathological features of bladder cancer patients, including T stage and recurrence. KIF23 deletion inhibits proliferation of mouse bladder cancer cells, stimulates apoptosis and inhibits tumor growth [33]. The heightened expression of KIF23 potentially contributes to the unrestrained proliferation of tumor cells, given its involvement in cell mitosis, ultimately fostering tumor growth and spread. Aligned with the literature review presented earlier, our research findings indicate a significant elevation of KIF23 expression in ACC, and a higher level of KIF23 expression is associated with a less favorable prognosis. Therefore, we hypothesize that KIF23 may play a role in the onset and progression of adenoid cystic carcinoma.

Furthermore, our Western blot (WB) immunoblotting experiments have confirmed expression of CCNA2 and KIF23 in ACC. The heightened molecular expression of CCNA2 and KIF23 correlates with the progression of ACC to more advanced stages. These genes can potentially serve as target genes for ACC treatment. This outcome provides scientific data and support for the prevention and treatment of ACC.

CONCLUSIONS

CCNA2 and KIF23 exhibit high expression levels in adenoid cystic carcinoma, suggesting their potential involvement in the development of the disease through inflammation and the regulation of immune cell. CCNA2 and KIF23 may be molecular targets for adenoid cystic carcinoma, and provide a basis for study of the mechanism of adenoid cystic carcinoma. The clinical significance of this medical research lies in advancing the medical field, enhancing clinical practices, elevating the standard of medical care, and ultimately promoting patient health, thereby exerting a profound and positive impact on society. The identification of new treatment methods or regimens resulting from this research can significantly enhance the efficacy of disease management, contributing to improved survival rates and enhanced quality of life for patients. Research can reveal the pathogenesis of diseases and provide more effective means for prevention and control. A deeper understanding of individual variations can pave the way for the development of more personalized treatment approaches, thereby enhancing treatment precision and minimizing unnecessary side effects. The improvement of medical diagnostic tools can diagnose diseases earlier and more accurately, and help to improve the timeliness and effect of treatment. It helps reduce overall costs to

the healthcare system through improved treatments, disease prevention, and diagnostic accuracy.

Abbreviations

ACC: adenoid cystic carcinoma; GEO: gene expression omnibus; DEGs: differentially expressed genes; WGCNA: weighted gene co-expression network analysis; PPI: protein–protein interaction; GSEA: Gene Set Enrichment Analysis; GO: gene ontology; KEGG: Kyoto Encyclopedia of Genes and Genomes; MAD: Median Absolute Deviation; STRING: Search Tool for the Retrieval of Interacting Genes; EMT: epithelial-mesenchymal transformation; CDK2: cyclin-dependent kinase 2; KIF23: Kinesin family member 23; MCC: Maximum Clique Centrality; MNC: Maximum Network Connectivity; ACC: adenoid cystic carcinoma group; ACC_OE: adenoid cystic oncogene overexpression group; ACC_KO: adenoid cystic oncogene knockout group.

AUTHOR CONTRIBUTIONS

Yongbin Di performed experiments mentioned in the paper, contributed to the work concept and design of the paper research, Haolei Zhang collected data, Bohao Zhang made statistical analysis of data, Tianke Li and Dan Li drafted the manuscript. Yongbin Di, Tianke Li and Dan Li revised the main content of the manuscript. All authors read and agree on the manuscript.

CONFLICTS OF INTEREST

The authors declare no conflicts of interest related to this study.

ETHICAL STATEMENT

All data was obtained from public databases, and therefore, ethical approval is not required.

FUNDING

No funding was used for this paper.

REFERENCES

1. Stell PM. Adenoid cystic carcinoma. Clin Otolaryngol Allied Sci. 1986; 11:267–91. https://doi.org/10.1111/j.1365-2273.1986.tb01928.x PMID:3028679

2. Coca-Pelaz A, Rodrigo JP, Bradley PJ, Vander Poorten V, Triantafyllou A, Hunt JL, Strojan P, Rinaldo A, Haigentz M Jr, Takes RP, Mondin V, Teymoortash A, Thompson LD, Ferlito A. Adenoid cystic carcinoma of the head and neck--An update. Oral Oncol. 2015; 51:652–61. https://doi.org/10.1016/j.oraloncology.2015.04.005 PMID:25943783

3. de Sousa LG, Neto FL, Lin J, Ferrarotto R. Treatment of Recurrent or Metastatic Adenoid Cystic Carcinoma. Curr Oncol Rep. 2022; 24:621–31. https://doi.org/10.1007/s11912-022-01233-z PMID:35212920

4. de Sousa LG, Jovanovic K, Ferrarotto R. Metastatic Adenoid Cystic Carcinoma: Genomic Landscape and Emerging Treatments. Curr Treat Options Oncol. 2022; 23:1135–50. https://doi.org/10.1007/s11864-022-01001-y PMID:35854180

5. Seo GT, Xing MH, Mundi N, Matloob A, Khorsandi AS, Urken ML. Adenoid Cystic Carcinoma of the Gingiva: A Case Report and Literature Review. Ann Otol Rhinol Laryngol. 2022; 131:1151–7. https://doi.org/10.1177/00034894211055591 PMID:34706573

6. Andreasen S. Molecular features of adenoid cystic carcinoma with an emphasis on microRNA expression. APMIS. 2018 (Suppl 140); 126:7–57. https://doi.org/10.1111/apm.12828 PMID:29924420

7. Kacew AJ, Hanna GJ. Systemic and Targeted Therapies in Adenoid Cystic Carcinoma. Curr Treat Options Oncol. 2023; 24:45–60. https://doi.org/10.1007/s11864-022-01043-2 PMID:36637743

8. Goh JJH, Goh CJH, Lim QW, Zhang S, Koh CG, Chiam KH. Transcriptomics indicate nuclear division and cell adhesion not recapitulated in MCF7 and MCF10A compared to luminal A breast tumours. Sci Rep. 2022; 12:20902. https://doi.org/10.1038/s41598-022-24511-z PMID:36463288

9. Hartsough EJ, Weiss MB, Heilman SA, Purwin TJ, Kugel CH 3rd, Rosenbaum SR, Erkes DA, Tiago M, HooKim K, Chervoneva I, Aplin AE. CADM1 is a TWIST1-regulated suppressor of invasion and survival. Cell Death Dis. 2019; 10:281. https://doi.org/10.1038/s41419-019-1515-3 PMID:30911007

10. Jiang A, Zhou Y, Gong W, Pan X, Gan X, Wu Z, Liu B, Qu L, Wang L. CCNA2 as an Immunological Biomarker Encompassing Tumor Microenvironment and Therapeutic Response in Multiple Cancer Types. Oxid Med Cell Longev. 2022; 2022:5910575. https://doi.org/10.1155/2022/5910575 PMID:35401923

11. Gao CT, Ren J, Yu J, Li SN, Guo XF, Zhou YZ. KIF23 enhances cell proliferation in pancreatic ductal adenocarcinoma and is a potent therapeutic target. Ann Transl Med. 2020; 8:1394. https://doi.org/10.21037/atm-20-1970 PMID:33313139

12. Sacks D, Baxter B, Campbell BCV, Carpenter JS, Cognard C, Dippel D, Eesa M, Fischer U, Hausegger K, Hirsch JA, Shazam Hussain M, Jansen O, Jayaraman MV, et al, and From the American Association of Neurological Surgeons (AANS), American Society of Neuroradiology (ASNR), Cardiovascular and Interventional Radiology Society of Europe (CIRSE), Canadian Interventional Radiology Association (CIRA), Congress of Neurological Surgeons (CNS), European Society of Minimally Invasive Neurological Therapy (ESMINT), European Society of Neuroradiology (ESNR), European Stroke Organization (ESO), Society for Cardiovascular Angiography and Interventions (SCAI), Society of Interventional Radiology (SIR), Society of NeuroInterventional Surgery (SNIS), and World Stroke Organization (WSO). Multisociety Consensus Quality Improvement Revised Consensus Statement for Endovascular Therapy of Acute Ischemic Stroke. Int J Stroke. 2018; 13:612–32. https://doi.org/10.1177/1747493018778713 PMID:29786478

13. Hay AJ, Migliacci J, Karassawa Zanoni D, McGill M, Patel S, Ganly I. Minor salivary gland tumors of the head and neck-Memorial Sloan Kettering experience: Incidence and outcomes by site and histological type. Cancer. 2019; 125:3354–66. https://doi.org/10.1002/cncr.32208 PMID:31174233

14. Jones AV, Craig GT, Speight PM, Franklin CD. The range and demographics of salivary gland tumours diagnosed in a UK population. Oral Oncol. 2008; 44:407–17. https://doi.org/10.1016/j.oraloncology.2007.05.010 PMID:17825603

15. Ellington CL, Goodman M, Kono SA, Grist W, Wadsworth T, Chen AY, Owonikoko T, Ramalingam S, Shin DM, Khuri FR, Beitler JJ, Saba NF. Adenoid cystic carcinoma of the head and neck: Incidence and survival trends based on 1973-2007 Surveillance, Epidemiology, and End Results data. Cancer. 2012; 118:4444–51. https://doi.org/10.1002/cncr.27408 PMID:22294420

16. Zhang S, Tischer T, Barford D. Cyclin A2 degradation during the spindle assembly checkpoint requires multiple binding modes to the APC/C. Nat Commun. 2019; 10:3863. https://doi.org/10.1038/s41467-019-11833-2 PMID:31455778

17. Fischer M, Quaas M, Steiner L, Engeland K. The p53-p21-DREAM-CDE/CHR pathway regulates G2/M cell cycle genes. Nucleic Acids Res. 2016; 44:164–74. https://doi.org/10.1093/nar/gkv927 PMID:26384566

18. Ruan JS, Zhou H, Yang L, Wang L, Jiang ZS, Wang SM. CCNA2 facilitates epithelial-to-mesenchymal transition via the integrin αvβ3 signaling in NSCLC. Int J Clin Exp Pathol. 2017; 10:8324–33. PMID:31966683

19. Jiang Y, Zhan H. Communication between EMT and PD-L1 signaling: New insights into tumor immune evasion. Cancer Lett. 2020; 468:72–81. https://doi.org/10.1016/j.canlet.2019.10.013 PMID:31605776

20. Gao T, Han Y, Yu L, Ao S, Li Z, Ji J. CCNA2 is a prognostic biomarker for ER+ breast cancer and tamoxifen resistance. PLoS One. 2014; 9:e91771. https://doi.org/10.1371/journal.pone.0091771 PMID:24622579

21. Aiello I, Fedele MLM, Román F, Marpegan L, Caldart C, Chiesa JJ, Golombek DA, Finkielstein CV, Paladino N. Circadian disruption promotes tumor-immune microenvironment remodeling favoring tumor cell proliferation. Sci Adv. 2020; 6:eaaz4530. https://doi.org/10.1126/sciadv.aaz4530 PMID:33055171

22. Gan Y, Li Y, Li T, Shu G, Yin G. CCNA2 acts as a novel biomarker in regulating the growth and apoptosis of colorectal cancer. Cancer Manag Res. 2018; 10:5113–24. https://doi.org/10.2147/CMAR.S176833 PMID:30464611

23. Li X, Ma XL, Tian FJ, Wu F, Zhang J, Zeng WH, Lin Y, Zhang Y. Downregulation of CCNA2 disturbs trophoblast migration, proliferation, and apoptosis during the pathogenesis of recurrent miscarriage. Am J Reprod Immunol. 2019; 82:e13144. https://doi.org/10.1111/aji.13144 PMID:31087423

24. Tadesse S, Anshabo AT, Portman N, Lim E, Tilley W, Caldon CE, Wang S. Targeting CDK2 in cancer: challenges and opportunities for therapy. Drug Discov Today. 2020; 25:406–13. https://doi.org/10.1016/j.drudis.2019.12.001 PMID:31839441

25. Liu TT, Li R, Huo C, Li JP, Yao J, Ji XL, Qu YQ. Identification of CDK2-Related Immune Forecast Model and ceRNA in Lung Adenocarcinoma, a Pan-Cancer Analysis. Front Cell Dev Biol. 2021; 9:682002.

https://doi.org/10.3389/fcell.2021.682002
PMID:34409029

26. Zhang J, Gan Y, Li H, Yin J, He X, Lin L, Xu S, Fang Z, Kim BW, Gao L, Ding L, Zhang E, Ma X, et al. Inhibition of the CDK2 and Cyclin A complex leads to autophagic degradation of CDK2 in cancer cells. Nat Commun. 2022; 13:2835. https://doi.org/10.1038/s41467-022-30264-0 PMID:35595767

27. Hu Y, Zheng M, Wang C, Wang S, Gou R, Liu O, Li X, Liu J, Lin B. Identification of KIF23 as a prognostic signature for ovarian cancer based on large-scale sampling and clinical validation. Am J Transl Res. 2020; 12:4955–76. PMID:33042400

28. Schmidt EE, Pelz O, Buhlmann S, Kerr G, Horn T, Boutros M. GenomeRNAi: a database for cell-based and in vivo RNAi phenotypes, 2013 update. Nucleic Acids Res. 2013; 41:D1021–6. https://doi.org/10.1093/nar/gks1170 PMID:23193271

29. Bai X, Cao Y, Yan X, Tuoheti K, Du G, Chen Z, Wu H, Guo L, Liu T. Systematic Pan-Cancer Analysis of KIF23 and a Prediction Model Based on KIF23 in Clear Cell Renal Cell Carcinoma (ccRCC). Pharmgenomics Pers Med. 2021; 14:1717–29. https://doi.org/10.2147/PGPM.S337695 PMID:35002290

30. Nislow C, Lombillo VA, Kuriyama R, McIntosh JR. A plus-end-directed motor enzyme that moves antiparallel microtubules in vitro localizes to the interzone of mitotic spindles. Nature. 1992; 359:543–7. https://doi.org/10.1038/359543a0 PMID:1406973

31. Li XL, Ji YM, Song R, Li XN, Guo LS. KIF23 Promotes Gastric Cancer by Stimulating Cell Proliferation. Dis Markers. 2019; 2019:9751923. https://doi.org/10.1155/2019/9751923 PMID:31007778

32. Zou JX, Duan Z, Wang J, Sokolov A, Xu J, Chen CZ, Li JJ, Chen HW. Kinesin family deregulation coordinated by bromodomain protein ANCCA and histone methyltransferase MLL for breast cancer cell growth, survival, and tamoxifen resistance. Mol Cancer Res. 2014; 12:539–49. https://doi.org/10.1158/1541-7786.MCR-13-0459 PMID:24391143

33. Yao DW, Song Q, He XZ. Kinesin family member 23 (KIF23) contributes to the progression of bladder cancer cells in vitro and in vivo. Neoplasma. 2021; 68:298–306. https://doi.org/10.4149/neo_2020_200803N808 PMID:33231086